141. Conformational Flexibility of the Methoxyphenyl Group Studied by Statistical Analysis of Crystal Structure Data

by **Wolfgang Hummel**[a]), **Karel Huml**[b]), and **Hans-Beat Bürgi**[a])*

[a]) Laboratorium für chemische und mineralogische Kristallographie, Universität Bern, Freiestr. 3, CH-3012 Bern

[b]) Institute of Macromolecular Chemistry, Czechoslovak Academy of Sciences, 16206 Prague 6, Czechoslovakia

(26.V.88)

In a large sample of observed methoxyphenyl groups, the twist angle τ about the MeO–C_{Ph} bond measuring internal rotation of the MeO group shows a continuous distribution with maxima at 0° (coplanar conformation) and ~ 90° (perpendicular conformation). The preferred conformation of methoxyphenyl depends on the nature of the *ortho*-substituents: In general, it is coplanar in the case of one or two *ortho*-hydrogens, and perpendicular in the case of two substituents. The internal rotation of the MeO group is accompanied by systematic variations in bond angles and bond distances: *1*) if MeO is twisted out of plane, the bond angle CH_3–O–C_{Ph} decreases from 117.7°, until it reaches a minimum of 114.9° at $\tau = \pm 90°$. The O–C–C angle which is *syn* to CH_3 for $\tau = 0°$ decreases from 124.6° to a minimum of 115.4° at $\tau = \pm 180°$. These angle changes keep the nonbonded distance $CH_3 \cdots$ *ortho* substituent maximal during internal rotation of MeO and tend to minimize the corresponding strain energy. *2*) In the perpendicular conformation, the O-atom is ~ 0.06 Å displaced from the Ph plane, O and CH_3 being on opposite sides of this plane. In addition, small but systematic increases of bond lengths MeO–C_{Ph} and CH_3–O are observed. These variations indicate a decrease in conjugation with increasing twist angle. Their interdependence during twisting and the magnitudes of the changes are close to values obtained by *ab initio* calculations.

Introduction. – In [1], the conformational flexibility of the acetoxyphenyl (AcOPh) group was studied by statistical analysis of crystal structure data. In the preferred conformation, the AcO group is perpendicular to the Ph ring. From an investigation of the methoxyphenyl (MeOPh) group, *Nyburg* and *Faerman* [2] found the coplanar conformation to be preferred, but they excluded molecules with non-hydrogen *ortho*-substituents from their survey. When such molecules are included, one may expect to find non-coplanar conformations as well. In this work, the conformational flexibility of the MeOPh fragment was studied using several methods of (multivariate) statistical analysis of crystal structure data. The results are discussed in terms of nonbonded interaction and conjugation effects.

Data Retrieval. – Crystal structures containing MeOPh groups *(Fig. 1)* were retrieved from the *Cambridge Structural Database* (*CSD*, version of May 1986 with 46750 entries in the connectivity file) [3]. The numbering scheme is adopted from the AcOPh fragment [1] in order to facilitate comparison between the two fragments. For the initial connectivity search, no restrictions were placed on the nature of the substituents at positions C(6) to C(10) *(Fig. 1)*. Atomic coordinates of 1244 structures were retrieved, and calculations of geometric parameters were performed. Names were assigned to geometrical parameters as follows: Dxy are bond distances (*e.g.* bond C(2)–O(4) is D24), Axyz are bond angles, and Txyzw are torsion angles. Twist deformation about the bond O(4)–C(5) is defined as in [4]:

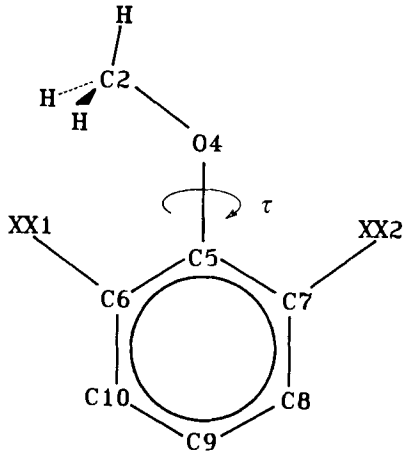

Fig. 1. *Atom types and numbering scheme in the MeOPh fragment.* XX1 and XX2 imply any type of substituent. The numbering scheme is adopted from the AcOPh fragment [1] in order to facilitate comparisons.

$$\tau = (\text{T2456} + \text{T2457} + 180)/2$$

Out of plane deformation at C(5) is defined as in [4]:

$$\chi = (\text{T2456} - \text{T2457} - 180)/2$$

The following test ranges were included in the geometry calculations: 1.40 Å ≤ D24 ≤ 1.60 Å, 1.30 Å ≤ D56, D57 ≤ 1.50 Å, and 115° ≤ A657 ≤ 130°. This avoids matching the search fragment with substructures of the same connectivity between non-H-atoms but different degrees of unsaturation [5]. In addition, structures were

Table 1. *Average Bond Lengths* [Å], *Bond Angles* [°], *and Torsion Angles* [°] (standard deviations of populations (σ_p) in parentheses; *N* is the number of fragments)

[a])	*N*	D24	D45	D56	D57	A245
Cluster 1	377	1.424(9)	1.367(10)	1.382(12)	1.397(15)	117.7(0.8)
Cluster 1[b])	214	1.423(9)	1.368(8)	1.383(12)	1.395(14)	117.7(0.8)
Cluster 2	103	1.428(11)	1.377(9)	1.393(17)	1.393(17)	114.9(1.6)
Cluster 2[b])	65	1.427(11)	1.376(7)	1.395(14)	1.395(14)	114.8(1.4)
From [2]	141	1.425(16)	1.371(15)	1.380(14)	1.391(17)	117.7(1.2)
From [6]		1.423(15)	1.361(15)	1.398(3)	1.398(3)	120.0(2.0)
	N	A456	A457	A657	τ	χ
Cluster 1	377	124.6(0.9)	115.4(0.9)	120.0(1.1)	0.0(8.8)	0.0(0.8)
Cluster 1[b])	214	124.6(0.8)	115.4(1.0)	120.1(1.1)	0.0(9.0)	0.0(0.9)
Cluster 2	103	120.0(1.6)	120.0(1.6)	120.0(1.6)	90.0(18.2)	1.5(0.9)
Cluster 2[b])	65	119.9(1.4)	119.9(1.4)	120.1(1.6)	90.0(18.2)	1.4(0.9)
From [2]	141	124.5(0.9)	115.2(1.1)	120.4(1.1)	–	–
From [6]		124	116	120	–	–

[a]) Cluster 1: $-45° < \tau \leq 45°$, cluster 2: $45° < \tau \leq 135°$.
[b]) $\sigma(\text{C–C})_{av} \leq 0.005$ Å.

considered only when all H-atoms at C(2) had been located in the crystal structure analysis. Entries with $R \geq 0.05$ or σ (C–C)$_{av} > 0.01$ Å and structures with error flags were rejected. The final list contains 480 MeOPh fragments in 261 structures. A list of reference codes [3] is available from the authors.

The same symmetry considerations as discussed for the AcOPh fragment [1] apply also for the MeOPh fragment. Choosing $0° \leq \tau < 90°$ as the asymmetric unit the following transformations and tests are necessary:

1) If T2456 < 0°, then change the signs of T2456 and T2457.

2) If |T2456 – T2457 – 180| > 180°, then subtract 360° from T2457 before calculating τ and χ. This test is necessary to get χ in the range of 0° and not around ±180° [4].

3) If $\tau > 90°$, then exchange D56 with D57 and A456 with A457, $\tau_{new} = 180° - \tau$.

Standard deviations of mean values (σ_m) are related to standard deviations of populations (σ_p, given in *Table 1*) by $\sigma_m = \sigma_p/\sqrt{N}$ where N is the number of data.

Univariate Analysis. – A histogram of τ *(Fig. 2)* shows a continuous distribution of twist angles with two symmetry-independent maxima. The absolute maximum is at $\tau = 0°$ (and due to symmetry at $\tau = 180°$) and a local, more diffuse one at $\tau = 80°$ (and due to symmetry at $\tau = 100°, -80°, -100°$). Before doing further statistical analyses, symmetry-independent clusters are chosen as follows: $-45° < \tau \leq 45°$ (cluster 1) and $45° < \tau \leq 135°$ (cluster 2).

Mean geometries calculated for the two clusters separately are given in *Table 1*. The main differences in bond distances are found for D45 between clusters 1 and 2 and for C–C bonds D56 and D57 within cluster 1. An additional calculation of means using a subset of very accurate data (σ(C–C)$_{av} \leq 0.005$ Å, *Table 1*) shows the same differences.

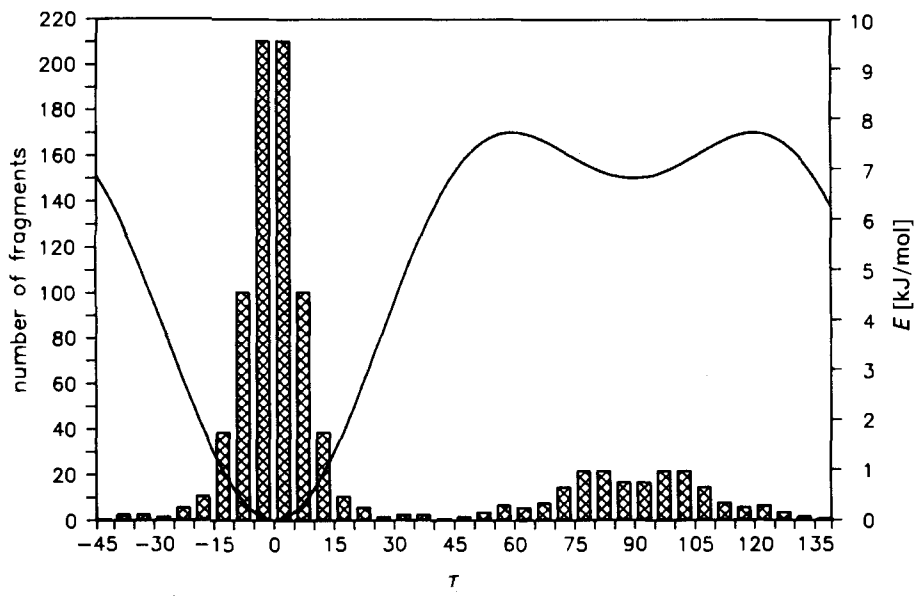

Fig. 2. *Histogram of twist angles τ in MeOPh fragments.* The solid line shows potential energy as a function of τ as obtained from *ab initio* calculations for anisole [10].

The variations in bond angles are much more pronounced. The difference in angle A245 between clusters 1 and 2 is 2.8°. The mean O–C–C angles A456 and A457 in cluster 1 differ by ±4.6° from 120°, the value of these angles in cluster 2, where A456 = A457 and D56 = D57 due to symmetry. In addition, cluster 2 shows the O-atom to be displaced from the Ph plane by $\chi = 1.5°$ for 0.060 Å, $\sigma_p = 0.005$ Å, O and Me being on opposite sides of this plane.

Mean values of structural parameters for cluster 1 *(Table 1)* are very close to those obtained by *Nyburg* and *Faerman* [2] and to those measured by electron diffraction for gaseous anisole [6] *(Table 1)*.

Multivariate Analysis. – The correlation matrix of each cluster was analyzed separately by factor analysis [7] in order to find local interrelations between the internal coordinates. Since the differences in the mean bond distances between the two clusters are small compared to the large scatter within each dataset, only the angles were included in this analysis. The results are shown in *Tables 2* and *3*.

In cluster 1, three eigenvalues are > 1, corresponding factors explain 73% of the total variance and are examined further. For most members of cluster 1, C(5) is very close to the plane of its three ligands and, therefore, the coordinates A456, A457, and A657 are linked by an equation of geometrical constraint, A456 + A457 + A657 = 360°. This leaves only two degrees of freedom for angular deformations (*e.g.* (2A657 – A456 – A457)/2 and (A456 – A457)/$\sqrt{2}$). These are represented by *Factors 1* and *2*. *Factor 2* also shows that a decrease of (A456 – A457) is correlated with an increase

Table 2. *Factor Analysis of Internal Coordinates for the MeOPh Group, Cluster 1* ($-45° < \tau \leq 45°$; coplanar conformation)

a) Factors

Factor	Eigenvalue	Percentage of variance	Cumulative percentage of variance
1	1.67	27.8	27.8
2	1.40	23.3	51.1
3	1.28	21.4	72.5
4	0.93	15.6	88.1
5	0.72	11.9	100.0
6	0.00	–	–

b) Components of internal coordinates[a])

Parameter	*Factor 1*		*Factor 2*		*Factor 3*	
	Component	Relative importance	Component	Relative importance	Component	Relative importance
A245	–0.03	–0.02°	0.44	0.36°	0.00	0.00°
A456	0.53	0.48°	–0.80	–0.73°	0.00	0.00°
A457	0.62	0.57°	0.75	0.69°	0.00	0.00°
A657	–1.00	–1.06°	0.02	0.02°	0.00	0.00°
τ	0.00	0.00°	0.00	0.00°	0.80	7.01°
χ	0.00	0.00°	0.00	0.00°	0.80	0.64°

[a]) The units are standard deviations. Multiplying each component by the standard deviation of the respective parameter (given in *Table 1*), the relative importance in [°] is obtained.

Table 3. *Factor Analysis of Internal Coordinates for the MeOPh Group, Cluster 2* ($45° < \tau \leq 135°$; perpendicular conformation)

a) Factors

Factor	Eigenvalue	Percentage of variance	Cumulative percentage of variance
1	2.18	36.3	36.3
2	1.57	26.2	62.5
3	1.30	21.7	84.2
4	0.55	9.1	93.3
5	0.40	6.7	100.0
6	0.00	–	–

b) Components of internal coordinates[a])

Parameter	*Factor 1*		*Factor 2*		*Factor 3*	
	Component	Relative importance	Component	Relative importance	Component	Relative importance
A245	0.00	0.00°	0.66	1.07°	0.54	0.88°
A456	−0.85	−1.40°	0.31	0.51°	−0.33	−0.56°
A457	0.85	1.40°	0.31	0.51°	−0.33	−0.56°
A657	0.00	0.00°	−0.71	−1.07°	0.71	1.07°
τ	0.86	15.66°	0.00	0.00°	0.00	0.00°
χ	0.00	0.00°	0.67	0.61°	0.52	0.47°

c) As above, after rotation of the factor axes (VARIMAX criterion)[a])

Parameter	*Factor 1*		*Factor 2*		*Factor 3*	
	Component	Relative importance	Component	Relative importance	Component	Relative importance
A245	0.00	0.00°	0.85	1.39°	−0.02	−0.04°
A456	−0.85	−1.40°	0.01	0.02°	−0.46	−0.76°
A457	0.85	1.40°	0.01	0.02°	−0.46	−0.76°
A657	0.00	0.00°	−0.07	−0.10°	1.00	1.51°
τ	0.86	15.66°	0.00	0.00°	0.00	0.00°
χ	0.00	0.00°	0.85	0.77°	−0.05	−0.04°

[a]) See *Footnote a, Table 2.*

of A245. *Factor 3* indicates a significant positive correlation between out of plane bending χ and twist angle τ, the proportionality constant being 0.091(= 0.64°/7.01°, see *Table 2b*).

In cluster 2, three eigenvalues are > 1, corresponding factors explain 84% of the total variance and will be considered further *(Table 3). Factor 1* shows that the O–C–C angle deformation (A456 – A457) is correlated with twist deformation τ, the proportionality constant being ±0.089 (= ±1.40°/15.66°, see *Table 3b*). The interpretation of *Factors 2* and *3* is not as obvious as for cluster 1 but can be simplified by rotating the factor axes (preserving orthogonality) as close as possible to some of the original internal parameter axes. After rotation (VARIMAX criterion [7]), many of the factor components become essentially zero *(Table 3c). Factor 2* now shows a positive correlation of A245 with the

out-of-plane bending χ, whereas *Factor 3* reveals the correlation of bond-angle changes at C(5) found also in *Factor 1* of cluster 1.

In cluster 2, symmetry requires that the mean values ⟨A456⟩ and ⟨A457⟩ as well as the correlations of A657 with A456 and A457 are equal. Cluster 1 has no such intrinsic symmetry, ⟨A456⟩ and ⟨A457⟩ differ by 9.2°. Interestingly, this does not affect the symmetry of the correlations of A657 with A456 and A457 *(Factor 1, Table 2)*. The ratios of the eigenvector components A456/A657 and A457/A657 are practically the same in both clusters.

Nonlinear Bivariate Analysis. – Factor analysis reveals only linear relationships between variables and is well suited to discern local correlations within clusters. Scatterplots of all variables against twist angle τ over the whole range of conformational space revealed significant nonlinear correlations which may be expressed in terms of empirical functions of τ. The analytic expressions and the respective numerical constants are chosen in such a way that they are consistent with the mean geometries of the clusters (*Table 1*) and the results of factor analyses (*Tables 2* and *3*).

The distribution of χ *vs.* τ has a sinusoidal shape *(Fig. 3)*. A two-parameter function was used to describe this shape (for a derivation see *Appendix*):

$$\chi = a \cdot b \cdot \sin\tau/(a^2 \cdot \sin^2\tau + b^2 \cdot \cos^2\tau)^{1/2} \quad (1)$$

where a is the slope at $\tau = 0°$ and b the maximum at $\tau = 90°$. The constant $a = 0.64°/7.01° \cdot 180°/\pi = 5.2°$ was taken from *Factor 3* of cluster 1 *(Table 2b)*, and $b = 1.5°$ is the mean value of χ in cluster 2 *(Table 1)*; the correlation coefficient is $r^2 = 0.61$, disregarding outliers (*Fig. 3*, dotted squares), it is $r^2 = 0.74$.

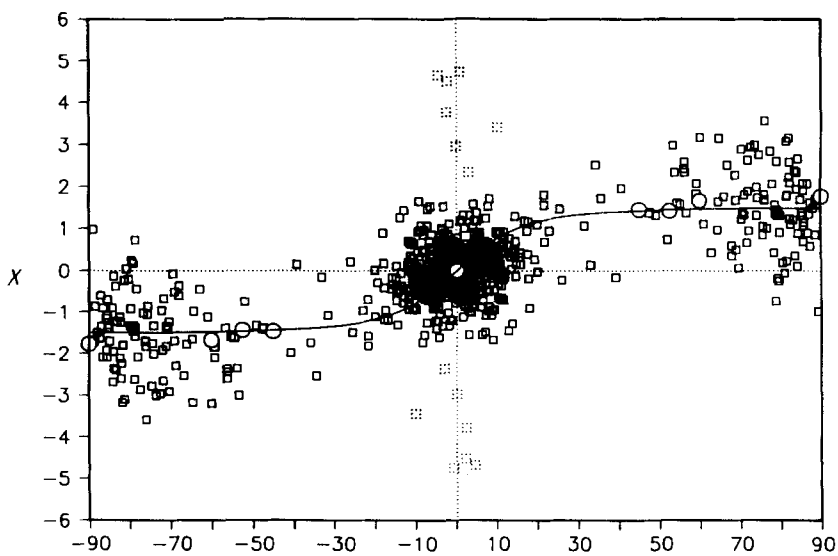

Fig. 3. *Scatterplot of twist angle* τ vs. *out-of-plane bending* χ. The outliers (dotted squares) are all cylophanes with nonplanar Ph rings (Refcodes [3]: BUZROD, DALTOZ, DALTUF). The solid line is calculated using *Eqn. 1*. The empty circles are from *ab initio* calculations on anisole [10].

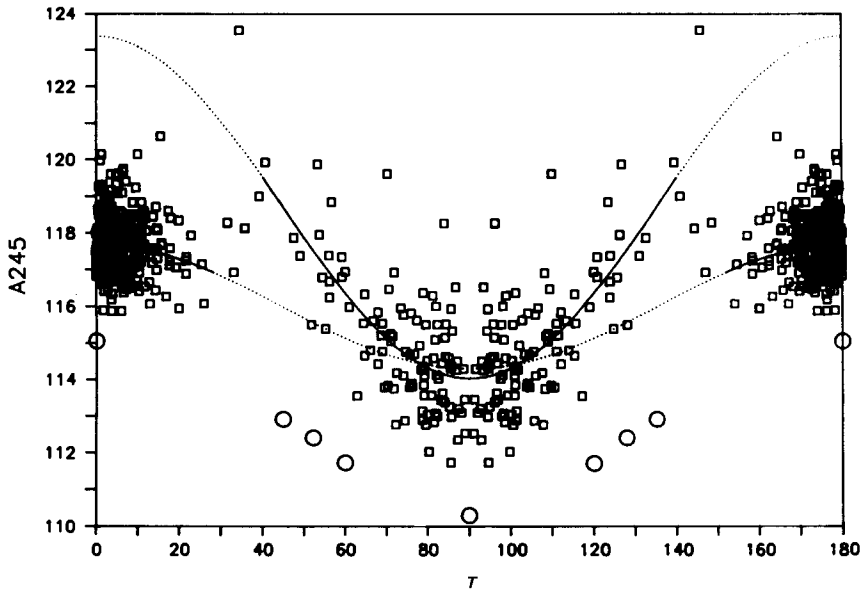

Fig. 4. *Scatterplot of twist angle* τ vs. *A245*. The lines are calculated from *Eqn. 2*. The solid lines show the range of regression analysis, the dotted lines are extrapolations. The empty circles are from *ab initio* calculations on anisole [10].

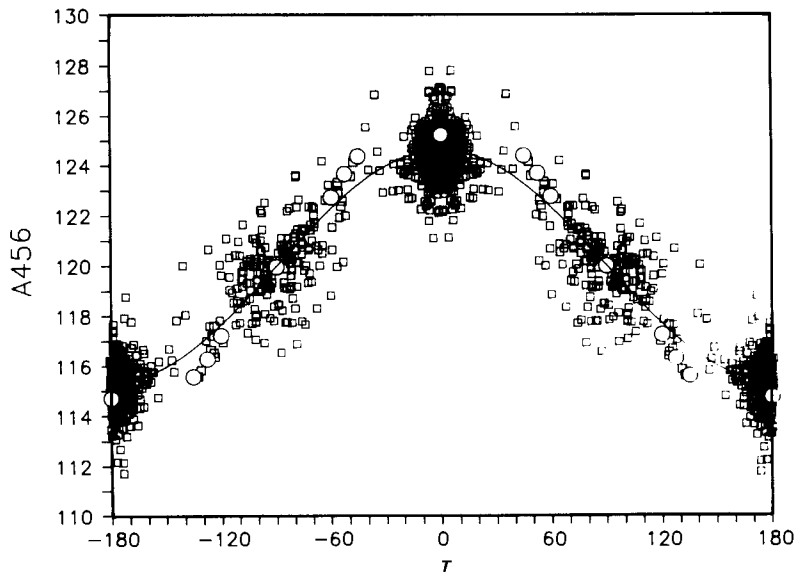

Fig. 5. *Scatterplot of twist angle* τ vs. *A456*. The solid line is calculated from *Eqn. 3* and the empty circles are from *ab initio* calculations on anisole [10].

The scatterplot of A245 *vs.* τ is more complex *(Fig. 4)*. Separate cosine functions:

$$A245 = a_0 + a_1 \cdot \cos(2\tau) \tag{2}$$

were fitted to the data. The ranges of regression and the fitted coefficients are: for cluster 1 $-30° < \tau < 30°$, $a_0 = 116.0$ (0.7)° and $a_1 = 1.68$ (0.69)°, $r^2 = 0.02$; for cluster 2 $40° < \tau < 140°$, $a_0 = 118.7$ (1.3)° and $a_1 = 4.66$ (0.53)°, $r^2 = 0.43$. In both cases, the solid lines in *Fig. 4* show the range of regression analysis, the dotted lines are extrapolations.

The variation of A456 with τ *(Fig. 5)* is best expressed by a cosine function

$$A456 = a_0 + a_1 \cdot \cos(\tau) \tag{3}$$

with $a_0 = 120.0$ (1.0)° and $a_1 = 4.63$ (4)°, $r^2 = 0.94$. The slope of *Eqn. 3* at $\tau = 90°$ is $-a_1 \cdot \pi/180 = -0.081$. The slope found from factor analysis on cluster 2 is −0.089 *(Table 3b, Factor 1)*.

The variations of bond distances with twist angle τ may also be approximated by cosine functions. Due to the relatively large scatter of data, these functions merely link the mean values of the different clusters and cannot be said to represent a continuous change in bond distances with twist angle. The functions are

$$D45 = a_0 + a_1 \cdot \cos(2\tau) \tag{4}$$

with $a_0 = 1.373(9)$° and $a_1 = -0.0057(6)$°, $r^2 = 0.17$ and

$$D56 = a_0 + a_1 \cdot \cos(\tau) \tag{5}$$

with $a_0 = 1.390(14)$° and $a_1 = -0.0071(5)$°, $r^2 = 0.16$.

Influence of *ortho*-Substituents. – To investigate the influence of *ortho*-substituents on the conformation of the MeOPh fragment, the data set of 480 fragments was divided into three subsets: XX1 = H = XX2 (126 fragments), XX1 = H ≠ XX2 (248 fragments), and XX1, XX2 ≠ H (106 fragments).

In the case of XX1 = H = XX2, the preferred conformation is coplanar, the distribution of τ is close to normal with a mean value of $\tau = 0°$ and $\sigma_p = 6.7°$ for $\tau < 40°$. One outlier at $\tau \approx 52°$ (Refcode [3]: CASNUF) was excluded.

The subset with one *ortho*-substituent (at XX2) shows a similar distribution of twist angles. Again the preferred conformation is a planar MeOPh group ($\tau = 0°, \sigma_p = 8.7°$ for $\tau < 90°$). Three fragments (Refcodes [3]: BUWMIP, CEPSHC, CORALY) out of 248 have a twist angle greater than 90° with the MeO group pointing towards the non-H substituent. The maximum twist angle observed is $\tau = 110.6°$. It seems remarkable that in all cases for which $\tau > 90°$ the *ortho*-substituent XX2 is a second MeO group.

The only significant difference in mean values of structural parameters between these two subsets and cluster 1 is found for the bond length D57: in the case of XX2 = H, it is 1.390 Å, $\sigma_m = 0.001$ Å, for XX2 ≠ H, it increases to 1.399 Å, $\sigma_m = 0.001$ Å. The other parameters differ by less than $2\sigma_m$ from each other and from the average values of cluster 1.

Mean parameter values for the subset with two *ortho*-substituents indicate a perpendicular conformation; they differ by less than $2\sigma_m$ from those of cluster 2. Two features of the distribution *(Fig. 6)* need further discussion: *1)* the filled bars seem to indicate a bimodal distribution with maxima at $\tau = 80°$ and $\tau = 100°$. To see, if this is a random

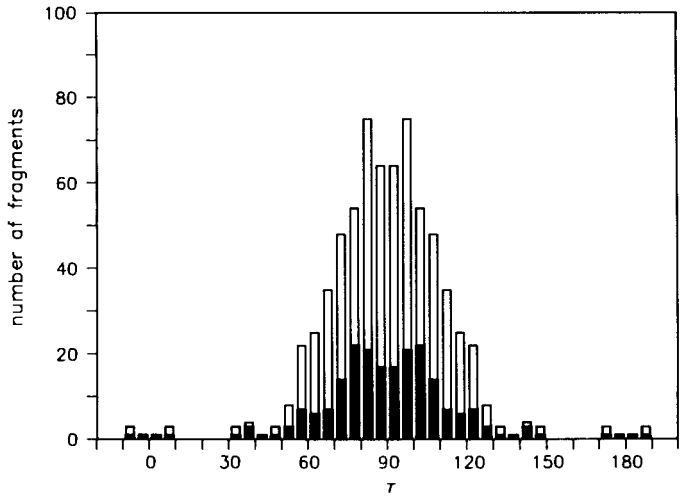

Fig. 6. *Histogram of twist angles τ for the case of two non-H* ortho-*substituents.* Filled bars represent structures with $R < 0.05$ and $\sigma(C-C)_{av} \leq 0.01$ Å and open bars structures without these restrictions.

effect due to the relatively small size of the sample an additional survey of the *Cambridge Database* was carried out for the subset XX1, XX2 ≠ H without restriction on *R* values. The result (348 fragments) is shown in *Fig. 6* as open bars. The bimodal shape of the distribution is now less obvious, but the maximum is still not at $\tau = 90°$. We interpret the distribution as being essentially monomodal and very broad with $\sigma_p = 20.7°$ (filled bars) or $\sigma_p = 19.2°$ (open bars) for $30° \leq \tau \leq 150°$. *2)* In the group XX1, XX2 ≠ H, four cases of coplanar conformations were found (*Fig. 6,* Refcodes [3]: BPELAM, BYAKAN, CUDVUS, ISPIMP). Inspection of these four structures revealed that in all cases the *ortho*-substituent on the side of the MeO group is part of a five-membered ring. No structures were found in the range $10° < \tau < 30°$. This supports the finding that the coplanar fragments belong to a special class of compounds.

Discussion. – The nonlinear bivariate statistical analysis has shown that internal rotation of the MeO group is accompanied by systematic variations in bond distances and bond angles. These and certain results from factor analysis may be rationalized in terms of two basic concepts, nonbonded interactions and conjugation effects.

1) If the twist angle τ decreases from $\tau = 90°$ to $\tau = 0°$, the angles A245 and A456 open up, A457 decreases and the distance D57 *trans* to the Me group increases (as expected from vibrational interaction force constants, for examples, see [8]). The angular changes partially compensate for the decrease in the nonbonded distance C(2)···XX1 due to twisting (*Fig. 7,* dotted line); they reflect minimization of strain energy during internal rotation of the MeO group. The magnitude of the changes depends on the nature of the *ortho*-substituents. This is seen most clearly in A245 *(Fig. 4)*. For XX1 = H = XX2, the mean angle at $\tau = 0°$ is ~ 118°, significantly smaller than for XX1 ≠ H ≠ XX2 for which extrapolation yields ~ 123°. This indicates a large nonbonded interaction between Me and the non-H *ortho*-substituents, as expected. The situation is different in the perpendicular conformation; the mean angle A245 (~ 115°) for fragments with non-H substi-

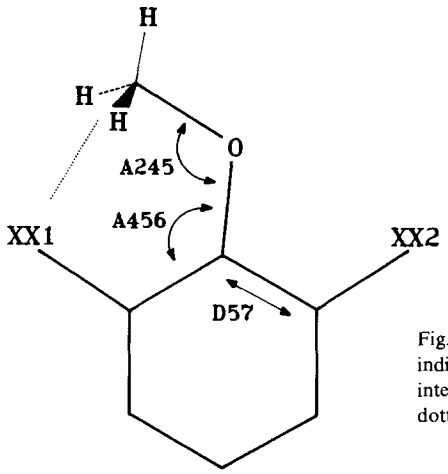

Fig. 7. *Coplanar conformation of the MeOPh fragment.* Arrows indicate the variations in bond angles and bond distances during internal rotation of the MeO group from $\tau = 90°$ to $\tau = 0°$. The dotted line shows the relevant nonbonded interaction.

tuents is the same as the (extrapolated) value for fragments with hydrogens indicating that for $\tau = 90°$ nonbonded interactions between the Me group and the *ortho*-substituents are independent of their nature. The four fragments mentioned earlier with XX1 ≠ H ≠ XX2 and coplanar conformation show A245 values in the same range as fragments with XX1 = H = XX2. In all four cases, XX1 (O or CH) is part of a five-membered ring and the C(2)···XX1 distance is, therefore, larger than in the other compounds with non-H substituents. The angles A456 and A457 show a smooth dependence on τ *(Fig. 5)*, and no influence of the nature of *ortho*-substituents can be seen.

For cluster 1, containing coplanar conformations only, A245 was found to increase when (A456–A457) decreases *(Table 2b, Factor 2)*. This also fits the same pattern of keeping the nonbonded distance C(2)···XX1 large.

2) In the perpendicular conformation, the angles A456 and A457 are equal *(Fig. 8)*, the C–O bond lengths are slightly but significantly longer than in the coplanar conformation (Δ(D24) = 0.004 Å, σ_m = 0.001 Å; Δ(D45) = 0.010 Å, σ_m = 0.001 Å) and atom O(4) is bent out of the Ph plane. The out-of-plane bending χ of O(4) tends to tilt the p-type orbital on C(5) towards the Me group and the sp^2 orbital on O(4) towards C(5); this improves their overlap. In the vicinity of the perpendicular conformation, an increase of χ is accompanied by an increase in A245 *(Table 3c, Factor 2)*. This increases the p character of the sp^2-type orbital at O(4) and the interaction with the p-type orbital on C(5). Both observations indicate some conjugation in the perpendicular conformation. Note that deformations improving this conjugation are coupled with a decrease of the angle A657 *(Table 3b, Factor 2)* in agreement with the results of *Domenicano* and *Vaciago* [9]. An interesting detail concerns the coupling of changes in τ, χ, and A456. *Fig. 8* shows that the out-of-plane deformation χ reaches more than 90% of its maximal value in the range $0 \leq \tau < 30°$. In the range $30° < \tau \leq 90°$, the main change apart from τ itself is in A456 (and A457). If we consider percentage deformations, τ lags behind χ in the first range, but is ahead of A456/A457 in the second. This indicates that the p(O(4))–p(C(5)) interaction is maintained as long as possible for $\tau < 30°$ and that the sp^2(O(4))–p(C(5)) interaction is established as quickly as possible for $\tau > 30°$.

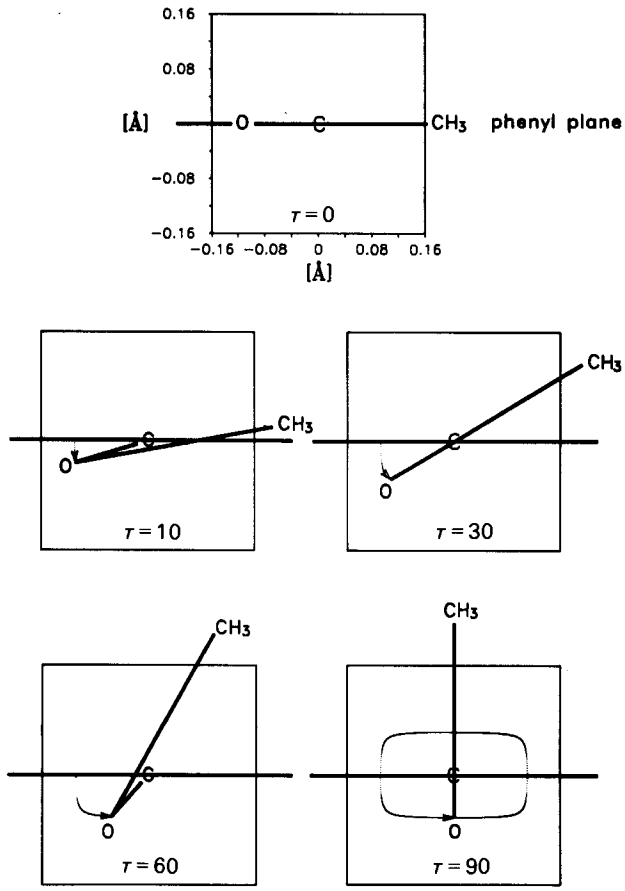

Fig. 8. *Projection of the MeOPh fragment parallel to the Ph plane showing the trajectory of O(4)* (dotted lines), *the bonds* $O-C_{Ph}$ *and* $O-CH_3$ *during internal rotation* τ *of the MeO group.* The scale (in Å) applies only inside the solid boxes.

The variations of the geometrical parameters during conformational interconversion derived statistically from anisole fragment structures are in the same direction and of the same order of magnitude as those calculated for anisole by fully optimized *ab initio* methods [10], as is seen from *Figs. 3–5* (empty circles). The calculated values for χ *(Fig. 3)* and A456 *(Fig. 5)* agree with the results of statistical analysis; the calculation underestimates the bond angle A245 *(Fig. 4)* and overestimates the bond distance D45 by an amount which is independent of the twist angle and, therefore, indicates a systematic deficiency of the *ab initio* calculations performed with a 4–21G basis set. Similar trends were found by *Konschin* [11] for the calculated C–O distances and C–O–H angles of phenol and catechol. Note that the curvature of the calculated potential is bigger at $\tau = 0°$ than at $\tau = 90°$ (*Fig. 2*, solid curve). This agrees qualitatively with the smaller width of the distribution at $\tau = 0°$ ($\sigma_p \approx 9°$) compared with that at $\tau = 90°$ ($\sigma_p \approx 18°$; *Table 1*). It has also been pointed out [12] that a perpendicular MeO group in *o*-dimethoxybenzenes shows a larger mean square displacement than a coplanar MeO group.

A previous study of the AcOPh fragment [1] showed a perpendicular conformation similar to that of the MeOPh fragment (cluster 2). In both fragments, a decrease of the twist angle is associated with an increase of A456 and A245, the degree of coupling being similar in the two cases. The out-of-plane bending is similar as well, 2.1° ($\sigma_m = 0.1°$) and 1.5° ($\sigma_m = 0.1°$), respectively. There is a significant difference in D45, 1.404 Å ($\sigma_m = 0.001$ Å) for the AcOPh fragment and 1.377 Å ($\sigma_m = 0.001$ Å) for the MeOPh fragment. The difference of 0.027 Å is similar to those for (alkyl)–O(alkyl) and (alkyl)–OCO(alkyl) fragments (0.025–0.032 Å). D45 is longer for the more electron-withdrawing substituent [13]. For the AcOPh fragment, it was found [1] that replacing a H-atom by a *ortho*-substituent will increase the associated C–C bond length (D56 and/or D57) by *ca.* +0.01 Å. A similar effect is seen in the MeOPh fragment: D57 for XX1 = H ≠ XX2 is 0.009 Å longer than D57 for XX1 = H = XX2.

In summary, statistical analysis of 480 MeOPh fragments has revealed differences in the coplanar and perpendicular conformations that are small but significant. The ranges of values for some structural parameters are several times larger than these differences, but the large size of the sample more than compensates for this fact. The width of the distributions for the two conformations and the correlation between changes in structural parameters give a faithful representation of many details of the conformational change if compared with results from *ab initio* calculations on anisole. Factor analysis has revealed subtle correlations between structural parameters indicative of electronic and steric properties of the fragment. Findings for the MeOPh and AcOPh fragments are consistent and show the expected chemical trends. The analyses for the two fragments impressively illustrate the power of statistical analysis of crystallographic structural data in uncovering overall patterns and fine details of conformational interconversions.

Appendix. – The parameter representation of a circle, $x^2 + y^2 = r^2$, with radius r is $x = r \cdot \cos\alpha$, $y = r \cdot \sin\alpha$. The analogous form for an ellipse, $x^2/a^2 + y^2/b^2 = 1$, is $x = c \cdot \cos\alpha$, $y = c \cdot \sin\alpha$ where $c = (x^2 + y^2)^{1/2}$ is the 'radius' at the angle α. Inserting x and y into the equation of the ellipse, we obtain $c^2 \cdot (\cos^2\alpha/a^2 + \sin^2\alpha/b^2) = 1$. Eliminating c from the parameter representation yields

$$x = a \cdot b/(a^2 \cdot \sin^2\alpha + b^2 \cdot \cos^2\alpha)^{1/2} \cdot \cos\alpha$$

$$y = a \cdot b/(a^2 \cdot \sin^2\alpha + b^2 \cdot \cos^2\alpha)^{1/2} \cdot \sin\alpha$$

The latter function was used to describe the sinusoidal function in *Fig. 3*. For $\alpha \to 0$, $\sin\alpha \to \alpha$, $\cos\alpha \to 1$, and $y \approx a \cdot \alpha$.

REFERENCES

[1] W. Hummel, A. Roszak, H.B. Bürgi, *Helv. Chim. Acta* **1988,** *71,* 1281.
[2] S.C. Nyburg, C.H. Faerman, *J. Mol. Struct.* **1986,** *140,* 347.
[3] F.H. Allen, S. Bellard, M.D. Brice, B.A. Cartwright, A. Doubleday, H. Higgs, T. Hummelink, B.G. Hummelink-Peters, O. Kennard, W.D.S. Motherwell, J.R. Rodgers, D.G. Watson, *Acta Crystallogr., Sect. B* **1979,** *35,* 2331.
[4] H.B. Bürgi, E. Shefter, *Tetrahedron* **1975,** *31,* 2976.
[5] P. Murray-Rust, J. Raftery, *J. Mol. Graph.* **1985,** *3,* 60.
[6] H.M. Seip, R. Seip, *Acta. Chem. Scand.* **1973,** *27,* 4024.
[7] SAS Institute Inc., SAS User's Guide: Statistics, 5th edn., Cary, NC: SAS Institute Inc., 1985, 621 pp.
[8] O. Ermer, S. Lifson, *J. Am. Chem. Soc.* **1973,** *95,* 4121.
[9] A. Domenicano, A. Vaciago, *Acta. Crystallogr., Sect. B* **1979,** *35,* 1382.
[10] M. Klessinger, A. Zywietz, *J. Mol. Struct.* **1982,** *90,* 341.
[11] H. Konschin, *J. Mol. Struct.* **1983,** *105,* 213; H. Konschin, *J. Mol. Struct.* **1983,** *92,* 173.
[12] G.M. Anderson III, P.A. Kollman, L.N. Domelsmith, K.N. Houk, *J. Am. Chem. Soc.* **1979,** *101,* 2344.
[13] F.H. Allen, A.J. Kirby, *J. Am. Chem. Soc.* **1984,** *106,* 6197.